ORBITAL DRAG NEAR SMALL BODIES DUE TO LOFTED FINES FROM SURFACE ACTIVITY

Matthew M. Wittal[1] and **Daniel Batcheldor**[2]
National Aeronautics and Space Administration
Deep Space Logistics
Kennedy Space Center, FL 32899

Abstract

Small bodies have been shown to be more granular and dusty than previously expected. Furthermore, as a result of landings, mining, or natural impacts, bodies with negligible atmospheres, such as moons and asteroids, may experience an exospheric environment abundant in lofted fines. Significant quantities of these may interfere with the nominal trajectories of spacecraft in low orbits. This work investigates the threshold of activity that would induce concerns to a spacecraft's nominal mission around various bodies including the Moon, Bennu, Comet Wild-2, and Phobos. Coupled motion of spacecraft navigation and control is expressed in $\mathsf{SE}(3)$.

Background

Natural processes generate lofted fines such as the ejection of material from comet tails due to varying temperatures from elliptical orbits [1], the electrostatic charging of fine particles from interaction with solar radiation [2], and unexplained volatility such as that observed on Bennu during the OSIRIS-REx mission [3]. Furthermore, natural impacts and human activities also have the potential to induce a dusty environment not just near the surface, but at significant altitudes from relatively high-velocity particles that remain in orbit for up to ten years [4, 5].

As the Artemis campaign begins a question has arisen as to how lofted and high-velocity dust may impact spacecraft performance, both as delivered contamination in the form of the Human Landing System up to the Gateway and as a source of orbital debris or even drag on the spacecraft if the density in orbit is great enough. Initial studies have demonstrated that a single landing event or impact does not induce enough of a hazard to be of concern to the Gateway during a nominal mission sequence, and is only a small concern for a satellite in Low Lunar Orbit (LLO) [6, 7]. It is the of interest to determine what amount of activity on the Moon or on other bodies such as Bennu, Phobos, or Lutetia, will induce a drag or torque on a spacecraft. Determination of a threshold of activity plays an important role in understanding risk and determining constraints such as attitude control, delta-V budget, and overall spacecraft health during maneuvers near small bodies.

[1]Robotics and Autonomous Systems Engineer, Granular Mechanics and Regolith Operations Laboratory & Deep Space Logistics, NASA Kennedy Space Center, FL, 32899 USA; Embry-Riddle Aeronautical University, 1 Aerospace Blvd., Daytona Beach, FL 32114, USA

[2]Southeastern Universities Research Association, Laboratory and Support Services Operations, NASA Kennedy Space Center, FL 32899 USA.

Methodology

To address this concern, we begin with the fundamentals laid out in [7] and expand upon them considering an arbitrary central body. For objects of interest such as the Moon and Phobos, considering the effects of Earth and Mars respectively is modeled using the N-body equation. However, particle velocities are determined and constrained based on the properties of the impactor or lander itself. Impactor dynamics have been sufficiently covered in previous work [8, 6] and landing dynamics covered by more recent studies [9, 7].

Current methodology considers the interaction between a particle and an asset in terms of their relative position (r_1 for the event, such as a landing or impact, and r_2 for the asset, such as a spacecraft). A potential derivation of orbital motion uses the following expressions:

$$r_1 = \frac{a(1-e^2)}{1+e\cos(f_o)} \tag{1}$$

$$r_2 = a(1+e) \tag{2}$$

where a is the semimajor axis, e is the eccentricity, and f_o is the initial true anomaly which can be solved by rearranging the equations

$$f_o = \pi - cos^{-1}(\frac{\vec{r_1}\cdot\vec{r_2}}{r_1 r_2}) \tag{3}$$

and

$$e = \frac{\frac{r_2}{r_1}-1}{\cos(f_o)+\frac{r_2}{r_1}} \tag{4}$$

However, maximum observed velocities due to an impactor approach $5\frac{km}{s}$ for fine particles [10], which is hyperbolic velocity for the moon, and thus these equations do not hold (they restrict $e<1$). We may consider the equivalent equations for hyperbolas:

$$r_1 = \frac{a(e^2-1)}{1+e\cos(f_1)} \tag{5}$$

and

$$r_2 = \frac{a(e^2-1)}{1+e\cos(f_2)} \neq p = a(e^2-1) \tag{6}$$

Consider that $f_2 = f_1 + \phi$ where ϕ is the difference between f_1 and f_2. Then the above equation can be rearranged to yield

$$e = \frac{\frac{r_1}{r_2}-1}{\cos(f_1+\phi)-\frac{r_1}{r_2}\cos(f_1)} = -\frac{1}{\cos[\frac{\pi}{2}+\tan^{-1}(\frac{b}{a})]} \tag{7}$$

We must then apply a conditional statement for hyperbolic velocities. We maintain the assumption that θ for small values of θ where θ is the Flight Path Angle (FPA). In that case, we can use the equation above for e, apply a conditional statement that:

```
if e > 1
```

$$a = \frac{r_1(1 + e\cos(f_1))}{e^2 - 1} \tag{8}$$

```
elseif e < 1
```

$$a = \frac{r_1(1 + e\cos(f_1))}{1 - e^2} \tag{9}$$

```
end
```

This has proven to work well (See Fig.1) for two-dimensional cases, but this work seeks to expand this to three-dimensional cases. Furthermore, non-spherical elements of the central body (especially for bodies such as Phobos and Itokawa, which are highly nonspherical) are also of interest to particle behavior in orbit and how this effects spacecraft rigid body dynamics.

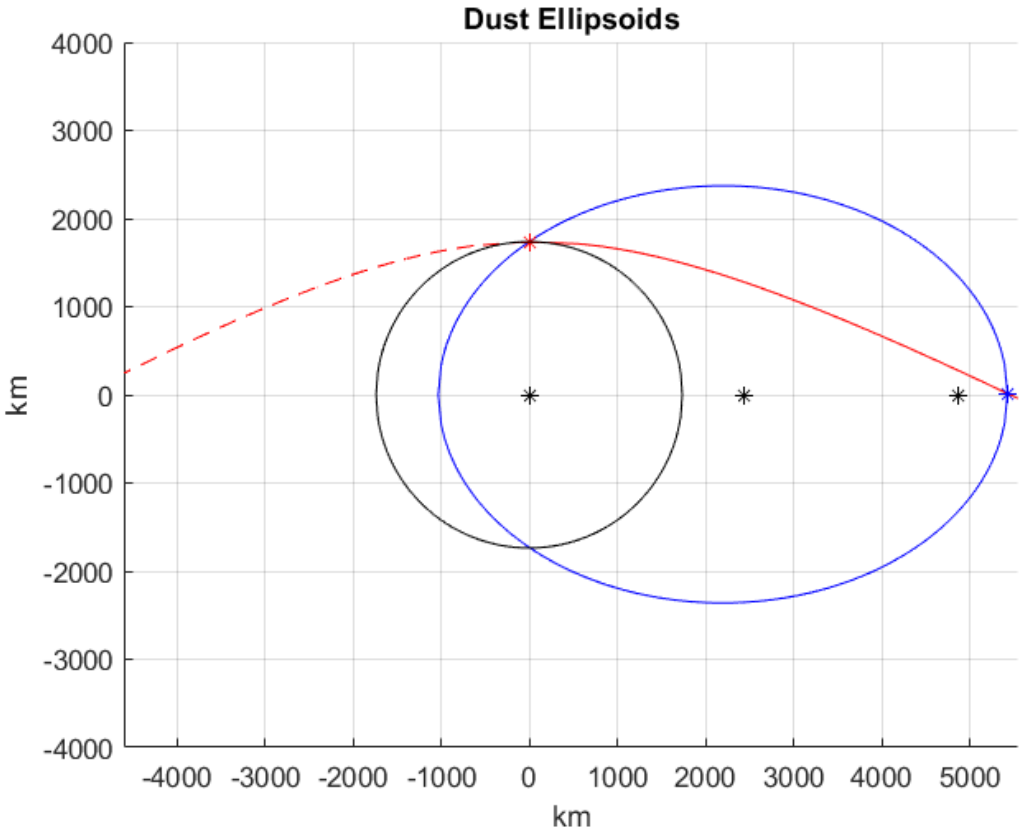

Figure 1. Dynamic relationship between the slowest particle and fastest particle able to intersect with an arbitrarily positioned spacecraft.

Rigid body dynamics for spacecraft motion are modeled using the $\mathsf{SE}(3)$ framework. The combined representation of attitude and position of a rigid body is called the "pose" can be modeled in as:

$$g = \begin{bmatrix} R & r \\ 0_{1\times 3} & 1 \end{bmatrix} \in \mathsf{SE}(3) \tag{10}$$

where $R \in \mathsf{SO}(3)$ is the attitude expressed as a rotation matrix which rotates from a rigid body frame $\mathcal{B}$ to some inertial frame $\mathcal{N}$ and r is the position vector in the inertial frame. The rigid body's velocity can be

defined using an augmented velocity vector $\mathbb{V}$ as

$$\mathbb{V} = \begin{bmatrix} \omega \\ v \end{bmatrix} \in \mathbb{R}^6 \tag{11}$$

such that $\omega \in \mathbb{R}^3$ is the angular velocity and $v \in \mathbb{R}^3$ is the velocity relative to the inertial frame and expressed in the body frame. The dynamics of a rigid body with a changing center of mass and moments of inertia in $\mathsf{SE}(3)$ are represented in the dynamic model as

$$\dot{g} = g\mathbb{V}^{\vee} \tag{12a}$$

$$\dot{\mathbb{V}} = \mathbb{I}^{-1}\left(\mathrm{ad}^*_{\mathbb{V}}\mathbb{I}\mathbb{V} + \tau + u\right) \tag{12b}$$

where

$$\mathbb{I} = \begin{bmatrix} J & 0_{3\times3} \\ 0_{3\times3} & mI_3 \end{bmatrix} \in \mathbb{R}^{6\times6}, \tag{13}$$

Here, $J \in \mathbb{R}^{3\times3}$ is the moment of inertia about the center of mass, and m is the mass of the body. The co-adjoint operator is defined as

$$\mathrm{ad}^*_{\mathbb{V}} = \mathrm{ad}^T_{\mathbb{V}} = \begin{bmatrix} -\omega^{\times} & -v^{\times} \\ 0_{3\times3} & -\omega^{\times} \end{bmatrix} \in \mathbb{R}^{6\times6} \tag{14}$$

such that the adjoint operator $\mathrm{ad}_{\mathbb{V}}$ is

$$\mathrm{ad}_{\mathbb{V}} = \begin{bmatrix} \omega^{\times} & 0_{3\times3} \\ v^{\times} & \omega^{\times} \end{bmatrix} \in \mathbb{R}^{6\times6} \tag{15}$$

For each time step, the mean direction of the oncoming ejecta particles must be rotated in to the body frame. The dust frame $\mathcal{E}$ is defined by its velocity relative to the central body's inertial frame.

$$R_{\mathcal{E}} = [\hat{v}_{\mathcal{E}}, \hat{p}_{\mathcal{E}}, \hat{h}_{\mathcal{E}}]$$

where $R_{\mathcal{E}}$ is the rotation matrix from the inertial frame to the dust frame and $\hat{v}_{\mathcal{E}}$ is the velocity unit vector for the ejecta.

$$\hat{h}_{\mathcal{D}} = \frac{\hat{v}_{\mathcal{E}} \times \hat{r}_{\mathcal{E}}}{||\hat{v}_{\mathcal{E}} \times \hat{r}_{\mathcal{E}}||} \tag{16}$$

is the angular momentum vector for the ejecta and $\hat{r}_{\mathcal{E}}$ is the position unit vector in the dust frame. Finally,

$$\hat{p} = \hat{v}_{\mathcal{E}} \times \hat{p}_{\mathcal{E}} \tag{17}$$

is the perpendicular vector relative to the mean ejecta velocity.

For each time step, the relative velocity may be determined by transforming the velocity of the incoming ejecta into the spacecraft body frame $\mathcal{B}$, and then determining both the external torque and drag based on the density of the ejecta and the cross-sectional area of the spacecraft in question.

Case Studies

Several case studies are considered in this work. We begin with a spacecraft in near-polar, low lunar orbit, and then generate an increasing number of landing events and simulations spaced over a long period of time, specifically the nominal Artemis timeline. Initial results of this simulation for a single landing event are shown in Fig. 2, while the depiction of the relative orbits are seen in Fig. 3. Although, as shown in [7], the impacts of these particles can be quantified and may be of concern in their own right. However, recent simulations show that the drag itself may cumulatively be an issue as well. Furthermore, the impact on rigid body dynamics for considerations such as pointing accuracy for LIDAR and the impact on fuel budget has yet to be quantified.

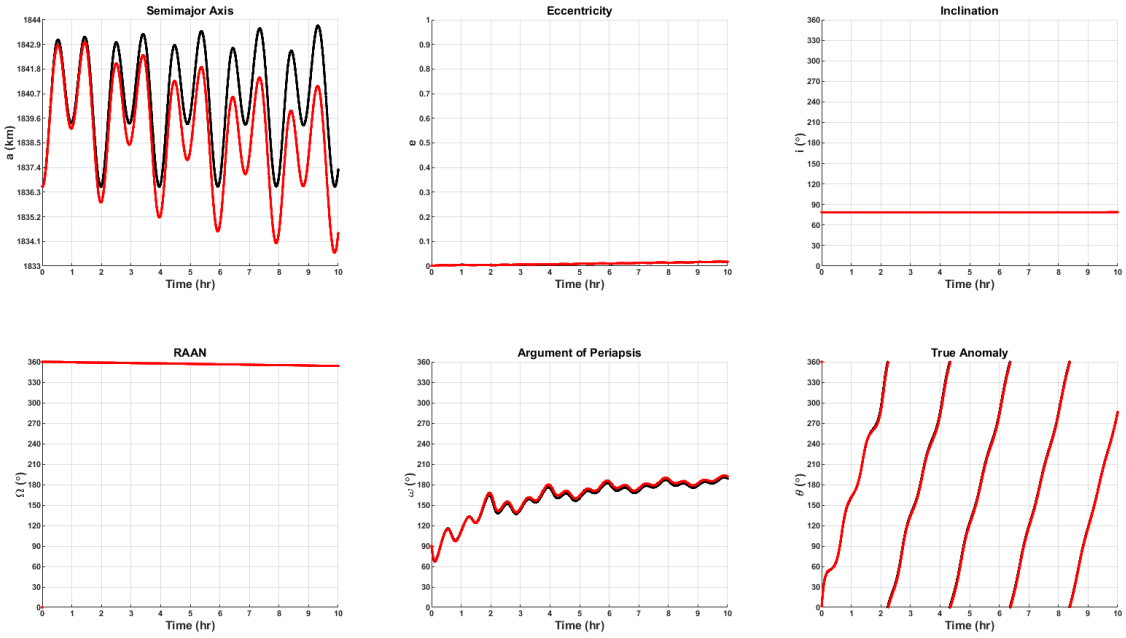

Figure 2. Classical orbital elements influenced by a single simulated landing event.

Within the scope of this work is the extension and generalization of this method to include other small bodies with a higher potential for ejecta mass such as Bennu, Lutetia, Itokawa, Comet Wild-2, and Phobos. For Bennu, Lutetia, and Wild-2, at least, there exists real world data to which simulations can be compared, such as particle density measurements from the tail of Wild-2 collected by the Stardust Sample Collection (SSC) instrument, [1], and surface data from Bennu [11] and Lutetia [12].

Thus it is the intent of this work to gain a better understanding of the effect of surface activities on various bodies on the pose of a spacecraft in orbit such that future mission design efforts can consider it into the design of the spacecraft, enabling a greater understanding and thus tolerance of such behavior.

Expected Results

Following the expansion on this first case study, future work will focus on decreasing the gravity of the central body to consider smaller objects of interest such as Bennu, Phobos, and Pan. In each case, projected surface conditions alter the estimated ejecta volume and particle distribution and thus alter the expected density of debris the spacecraft is projected to encounter. Consideration of rigid body dynamics also means that not only drag, but torque can also be modeled.

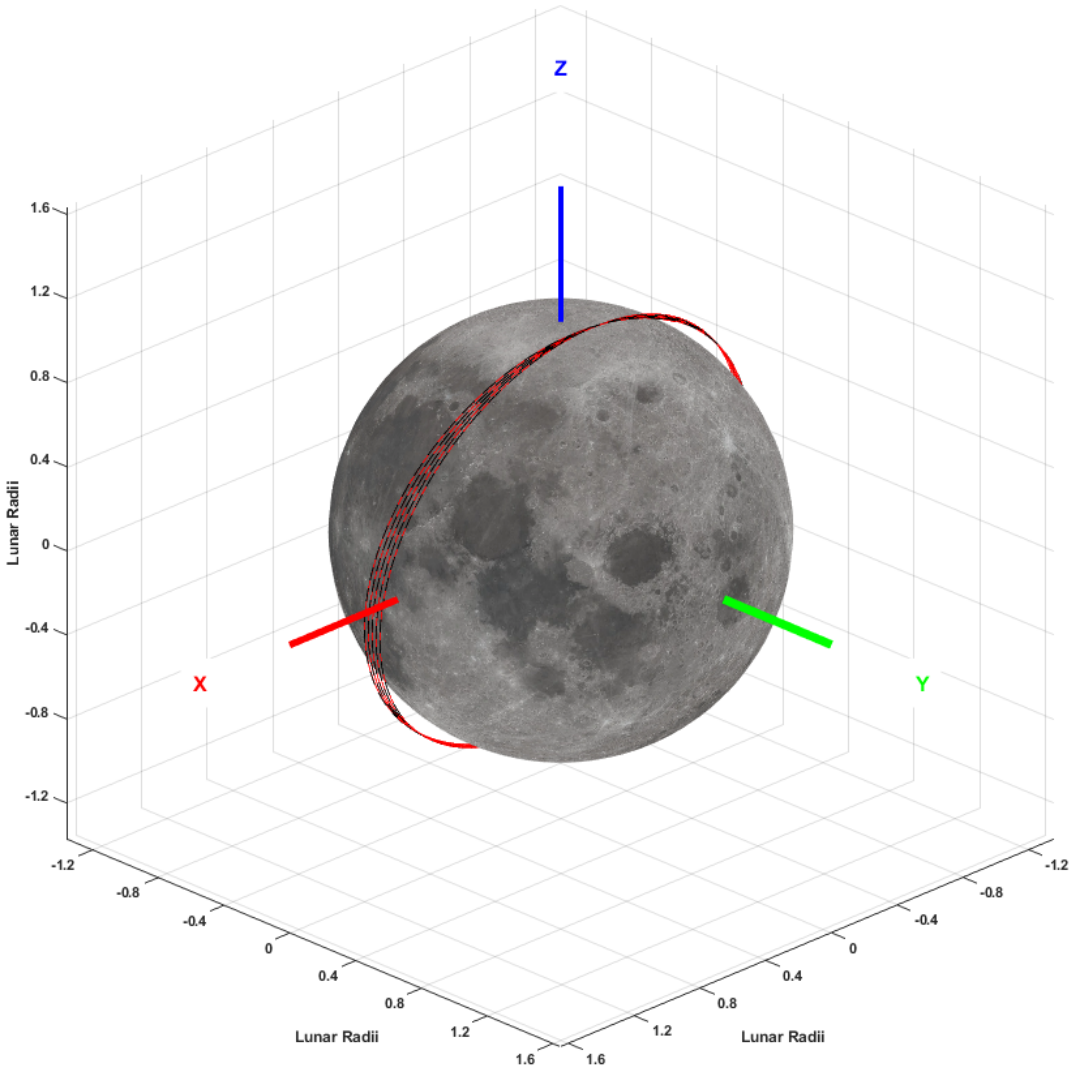

Figure 3. The inclination of the orbit mimics what could be expected from a descent element or communications satellite.

References

[1] M. S. Kelley, W. T. Reach, and D. J. Lien, "The dust trail of comet 67p/churyumov–gerasimenko," *Icarus*, vol. 193, no. 2, pp. 572–587, 2008. Saturn's Icy Satellites from Cassini.

[2] J. R. P. III, H. Wang, A. Hillegass, A. Esparza, A. R. Dove, and T. A. Elgohary, "Implementation of charged particle behavior in discrete element method (dem) simulations," in *ASCE Earth and Space Conference 2021*, 2021.

[3] D. S. Lauretta, C. W. Hergenrother, S. R. Chesley, *et al.*, "Episodes of particle ejection from the surface of the active asteroid (101955) bennu," *Science*, vol. 366, no. 6470, p. eaay3544, 2019.

[4] M. Wittal and R. Powers, "Spaceflight hazards of escape-velocity-domain impact ejecta in the cr3bp," in *2019 AAS/AIAA Astrodynamics Specialist Conference*, 2019.

[5] J. E. Lane and P. T. Metzger, "Ballistics Model for Particles on a Horizontal Plane in a Vacuum Propelled by a Vertically Impinging Gas Jet," *Particul. Sci. Tech.*, vol. 30, no. 2, pp. 196–208, 22012.

[6] P. M. M.M. Wittal, J.R. Phillips *et al.*, "Behavior of high-velocity dust generated by lander plumes in the lunar environment," in *2020 AAS/AIAA Astrodynamics Specialist Conference*, 2020.

[7] M. Wittal and S. Butts, "System-level model-based risk determination for lunar mission design," in *21st IAASS Conference*, 2021.

[8] K. H. K.R. Housen, "Ejecta from Impact Craters," *Icarus*, vol. 211, pp. 856–875, 2011, 10.1016/j.icarus.2010.09.017.

[9] P. Metzger, "Dust transport and its effects due to landing spacecraft," in *2020 Lunar Dust Workshop*, 2020.

[10] G. Gladstone, D. Hurley, K. Rutherford, *et al.*, "Lro-lamp observations of the lcross impact plume," *Science*, vol. 330, pp. 472–476, 2010, doi:10.1126/science.1186474.

[11]

[12] A. Coradini, F. Capaccioni, *et al.*, "The surface composition and temperature of asteroid 21 litetia as observed by rosetta/virtis," *Science*, vol. 334, no. 6055, pp. 492–494, 2011.